

# DESIGN AND PERFORMANCE OF A MICROELECTROMAGNETIC VIBRATION-POWERED GENERATOR.

S. P. Beeby<sup>1</sup>, M. J. Tudor<sup>1</sup>, E. Koukharenko<sup>1</sup>, N. M. White<sup>1</sup>, T. O'Donnell<sup>2</sup>, C. Saha<sup>2</sup>, S. Kulkarni<sup>2</sup>, S. Roy<sup>2</sup>

<sup>1</sup>University of Southampton, School of Electronics and Computer Science, Southampton SO17 1BJ, UK.

<sup>2</sup>Tyndall National Institute, Prospect Row, Cork, Ireland.

## ABSTRACT

*In this paper we report on the design, simulation and initial results of a microgenerator, which converts external vibrations into electrical energy. Power is generated by means of electromagnetic transduction with static magnets positioned either side of a moving coil located on a silicon structure designed to resonate laterally in the plane of the chip. In this paper the development and fabrication of a micromachined microgenerator that uses standard silicon based fabrication techniques and low cost, batch process is presented. Finite element simulations have been carried out using ANSYS to determine an optimum geometry for the microgenerator. Electromagnetic FEA simulations using Ansoft's Maxwell 2D software have shown voltage levels of 4 to 9V can be generated from the single beam generator designs. Initial results at atmospheric pressure yield  $0.5\mu\text{W}$  at  $9.81\text{ms}^{-2}$  and 9.5 kHz and emphasise the importance of reducing unwanted loss mechanisms such as air damping.*

## INTRODUCTION

Wireless sensor networks using low power Zigbee or IEEE 802.15.4 protocols avoid the use of expensive, potentially unreliable and inconvenient wired connections that can restrict applications. Wireless solutions offer flexibility, ease of implementation and can lead to the placement of sensors in previously inaccessible locations. This flexibility offers significant advantages in many applications such as condition based monitoring (CBM) [1]. Low-power design has become one of the most important requirements in both electronic and sensor design. Low power Microelectromechanical Systems (MEMS) have been combined with wireless sensor solutions in numerous applications, for example, health care, industrial, structural (embedded sensors in building and bridges), consumer products, and defence [2]. In such applications the energy necessary to power the sensor node is typically stored in batteries. These contain a finite amount of energy, tend to be bulky, have a limited shelf life and limited temperature range. The inherent low power nature of these applications presents an opportunity

for alternative power sources which can potentially replace, or at least augment, batteries.

Renewable power supplies convert energy from an existing source available in the application environment (e.g. light, thermal, kinetic and even nuclear energy) into electrical energy. Kinetic energy generators generate electrical energy from movement present in the application environment. The kinetic energy is typically present in the form of vibrations, random displacements or forces within the environment. There are many potential applications where such energy sources are present including common household goods, industrial plant and equipment, moving structures such as automobiles and aeroplanes, stationary structures such as buildings and bridges [3] and human based applications [4 5]. The amount of energy generated by this approach depends fundamentally upon the amount and form of the kinetic energy available in the application environment and the efficiency of the generator and the power conversion electronics. Kinetic energy can be harvested by using piezoelectric materials, electromagnetic or electrostatic transduction mechanisms [6 7 8].

This paper presents details of the design and fabrication of an electromagnetic MEMS microgenerator that uses standard silicon-based fabrication techniques and low cost, batch processes.

## MEMS ELECTROMAGNETIC GENERATOR

The envisaged arrangement for the MEMS version of a device based on four magnets is shown in figure 1. The coil is located on a silicon cantilevered paddle, designed to vibrate laterally in the plane of the wafer. Magnets are positioned within etched recesses in Pyrex wafers, which are then bonded to each face of the silicon layer. The bonding process is aligned to ensure correct placement of the coil relative to the magnets. The paddle is realised by deep reactive ion etched (DRIE) through the thickness of the wafer. Figure 2 shows the top view of the silicon paddle layer.

The mechanical characteristics of the dynamic component of the generator have been simulated using ANSYS finite element analysis (FEA). The natural frequencies of different cantilever dimensions (each 1mm long, 0.5mm thick, in model A the beam is 500 $\mu\text{m}$  wide, B 400 $\mu\text{m}$  wide and C 300 $\mu\text{m}$  wide) have been determined using a modal analysis. The optimum mode is the

fundamental lateral vibration in the plane of the wafer. The amplitude of vibration is limited by the surrounding silicon frame, which limits the displacement of the centre point of the coil to  $240\mu\text{m}$ . The device frame forms a physical over-range protection by limiting the motion of the paddle.

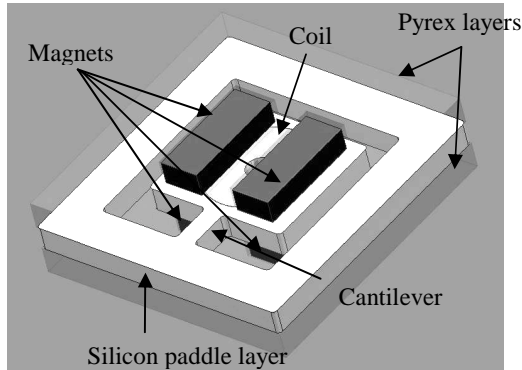


**Fig. 1.** Micromachined silicon generator

### ANALYTICAL MODELLING

The amount of power generated by an electromagnetic resonant generator can be calculated from equation 1 where  $m$  is the inertial mass,  $a$  the input acceleration,  $\omega_{res}$  the resonant frequency of the generator and  $Q_{o/c}$  the open circuit Q-factor.

$$P = \frac{ma^2}{8\omega_{res}} Q_{o/c} \quad (1)$$

Our design has a silicon inertial structure  $3.7\text{mm}$  wide,  $3\text{mm}$  long with a discrete copper coil of  $2.4\text{mm}$  outer diameter and  $0.6\text{mm}$  inner diameter and a mass of  $0.028\text{g}$ . The predicted power output versus frequency for a fixed acceleration of  $9.81\text{ms}^{-2}$  is shown in figure 2. For a fixed acceleration, excitation amplitude decreases with frequency<sup>2</sup> and therefore the power decreases with frequency. For micromachined devices the value of  $Q_{o/c}$  will depend greatly on air damping effects and it is essential the generator is operated in a vacuum to avoid excessive losses. Equation 1 predicts  $52\mu\text{W}$  for a resonant frequency of  $1\text{kHz}$  at  $9.81\text{ms}^{-2}$  and a Q of 1000, of which  $26\mu\text{W}$  can be harvested assuming a matched load. This equates to an inertial mass displacement of  $250\mu\text{m}$  which is half the permissible range of travel. Doubling this to the full  $500\mu\text{m}$  distance produces 4 times the available power,  $208\mu\text{W}$ . The following section on magnetic modelling discusses the influence of the resistive load on the damping and therefore the inertial mass

displacement and simulates the resulting voltage and power output.

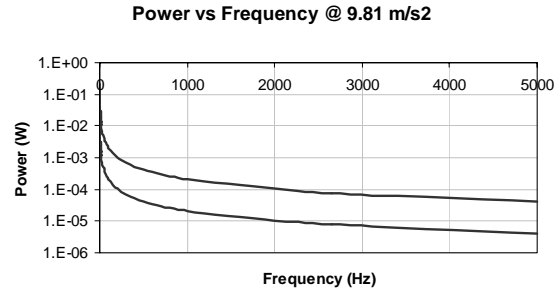


**Fig. 2.** Power output vs. frequency for  $9.81\text{ms}^{-2}$  acceleration

### MAGNETIC MODELLING

Electromagnetic FEA simulations using Ansoft's Maxwell 2D software have also been performed to determine the voltages which can be generated from the single beam generator designs. The coil used in the generator is a circular wire wound enamelled copper coil with 600 turns of  $25\mu\text{m}$  diameter wire. The dc resistance of the coil is  $112\Omega$  and the inductance is  $367\mu\text{H}$  measured at  $10\text{kHz}$ . The resulting mass of the silicon paddle plus coil is calculated to be  $0.028\text{g}$ . As described above the coil is to be sandwiched between magnets. Four magnets, with opposite polarity, are placed so as to form a two pole arrangement, two magnets, with opposite polarity, are placed above and two magnets below the coil, to form the two poles of opposite polarity as in figure 3. The magnets used are sintered NdFeB.

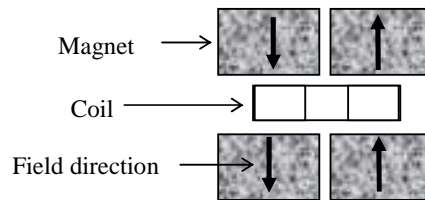


**Fig. 3.** Magnet configuration used in the simulation.

3D FEA simulation has been used to verify the flux density distribution between the magnets. The flux density distribution for the two pole configuration is shown in figure 4. As can be seen from the plot the flux density varies from approximately  $+0.5\text{T}$  under one pole to approximately  $-0.5\text{T}$  under the other pole.

In order to determine the voltage which would be induced in the coil, given a certain vibration frequency,  $f$ , coil displacement,  $X_{max}$ , and velocity,  $v$ , a 2D transient finite element simulation is used. A sinusoidal velocity

given by  $v = X_{\max} 2\pi f \sin(2\pi ft)$ , is used as input to the transient simulation to specify the coil movement.

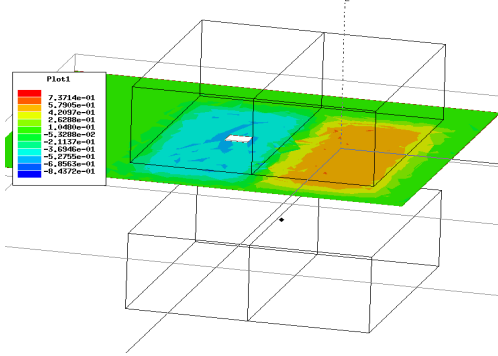


**Fig. 4.** 3D FEA simulation of flux density for the two pole configuration.

Table 1 gives the predicted results for the voltages and powers generated according to the FE simulation for all three beam geometries, and both magnet configurations for a 240  $\mu\text{m}$  coil displacement.

Model	$f_{\text{res}}$ (kHz)	$R_{\text{load}}$ (k $\Omega$ )	$V_{\text{load}}$ (V)	$P_{\text{load}}$ (mW)
A	9.812	20.4	9.0	2.0
B	7.149	14.8	6.5	1.45
C	4.743	9.8	4.3	0.96

Table 1. Simulation results for the natural frequency,  $f_{\text{res}}$ , voltages,  $V_{\text{load}}$ , (peak) and power,  $P_{\text{load}}$ , delivered to the load resistance,  $R_{\text{load}}$  for three generator structures.

In contrast to many micro-fabricated magnetic generator structures, the simulation results indicate that reasonable voltages can be generated. The estimated power is based on the power delivered to the load resistance indicated in the table. This value of load resistance has been chosen so as to maximise displacement for 9.81ms<sup>-2</sup> vibration acceleration as described in the following section.

For the purposes of the 2D finite element simulation the maximum displacement is fixed at 240  $\mu\text{m}$  and it is assumed that sufficient mechanical force, given by the product of mass and acceleration, exists to give the required displacement. In order to illustrate how this is affected by the choice of load resistance, we assume that the motion of the device can be described as a single degree of freedom, damped mass-spring system. If we assume that the device is operated at resonance, i.e. the frequency of the driving vibration is equal to the natural frequency of the device, then it can be shown that the amplitude of the movement of the mass is given by [4];

$$X_{\max} = \frac{ma}{D2\pi f_{\text{res}}} \quad (2)$$

where,  $D$  is the electromagnetic damping factor for the device. In this case only electromagnetic damping is considered, and the electromagnetic damping factor,  $D$  can be estimated by

$$D = \frac{(NlB)^2}{R_{\text{load}} + R_{\text{coil}} + j\omega L_{\text{coil}}} \quad (3)$$

where  $N$  is the number of turns in the generator coil,  $l$  is the side length of the coil (assumed square), and  $B$  is the flux density to which it is subjected and  $R_{\text{load}}$ ,  $R_{\text{coil}}$ , and  $L_{\text{coil}}$  are the load resistance, coil resistance and coil inductance respectively. The expression in (3) is really only valid for the case where the coil moves from a high field region  $B$ , to a zero field region. Therefore it is not an exact expression for the structure used here, and a more exact value for the electromagnetic damping should be determined from the finite element analysis. However, equation (3) does show that the damping factor depends of the load resistance, given that all the other parameters are fixed by the geometry of the device. The expression in (2) shows that the maximum displacement is inversely proportional to the damping factor, and proportional to the input acceleration. The other parameters in (2) are fixed by the device geometry. If the input acceleration is fixed at a value of 9.81ms<sup>-2</sup>, then the maximum displacement can be controlled by choosing the value of load resistance,  $R_{\text{load}}$ . The value of load resistance shown in table 1 corresponds to the value required to achieve a 240  $\mu\text{m}$  displacement of the paddle for a 9.81ms<sup>-2</sup> acceleration input.

## ASSEMBLY AND TESTING

The fabrication process involves evaporating and patterning aluminium contact pads and then deep reactive ion etching (DRIE) the generator profile through the wafer. The fabrication process is discussed in more detail elsewhere [9]. For the purposes of this generator the magnets have been mounted in conventionally machined Perspex chips. The assembly process consists of bonding the coil into the silicon paddle (see figure 5), attaching two permanent magnets inside of the cavity of each Perspex chip and assembling the Perspex chips either side of the silicon die with the magnets aligned over the centre of the coil. Finally, ferrous keepers are glued to the magnets to complete the magnetic circuit. The assembled device packaged for initial tests is shown in figure 6. The chip size is 5.7 x 6mm and the whole volume is 100mm<sup>3</sup>.

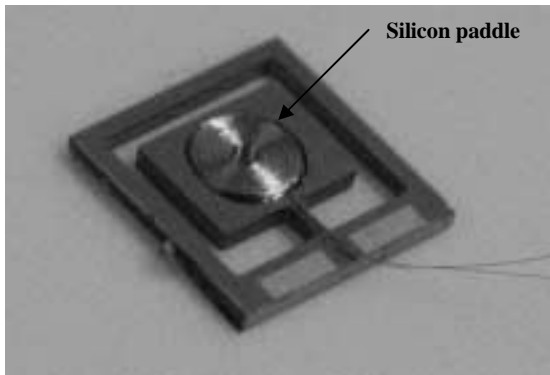


**Fig. 5.** Cu-coil integrated in the silicon paddle



**Fig. 6.** Assembled microgenerator

Initial testing at atmospheric pressure has yielded 21nW at  $1.92\text{ms}^{-2}$  rms at 9.5kHz into a matched load. If scaled up to  $9.81\text{ms}^{-2}$  the quadratic relationship predicts 0.5 $\mu$ W. The results however clearly show the importance of operating these devices in a vacuum in order to increase  $Q_{o/c}$  and obtain higher levels of amplitude at resonance and therefore increased power.

### CONCLUSIONS

This work presents the results of the mechanical and electromagnetic behaviour of a silicon vibration-powered generator.

Two dimensional transient finite element simulations have been performed in order to investigate the magnitude of voltages that can be generated. Finite element simulation predicts that voltage levels 4 to 9 V can be generated for a full displacement of the paddle.

These voltages can be generated for a  $9.81\text{ms}^{-2}$  acceleration input, with an optimised choice of load resistance. Initial experimental results show much lower powers but these are performed at atmospheric pressure where air damping will dominate the device.

### REFERENCES

- [1] K. Bult, A. Burstein, D. Chang, M. Dong, M. Fielding, J. Ho, W. J. Kaiser, E. Kruglick, F. Lin, T H. Lin, H. Marcy, R. Mukai, P. Nelson, K. S. J. Pister, G. Pottie, H. Sanchez, O. M. Stafsudd, K. B. Tan, C. M. Ward, S. Xue, and J. Yao, "A Distributed, Wireless MEMS Technology for Condition Based Maintenance," Proc. of the 1996 Integrated Monitoring, Diagnostics and Failure Prevention Conference, Society of Machine Failure Protection Technology (MPFT), pp. 373-80, Mobile, Alabama, USA, 24 April 1996.
- [2] K. Najafi, "Low-power Micromachined Microsystems, IEEE, Proc. 1<sup>st</sup> Int. Symp on Low Power Electronics and Design, pp.1-8, July 2000.
- [3] S. Roundy, P.K. Wright, J. Rabaye, "A study of low level vibrations as a power source for wireless sensor nodes," Computer Communications **26**, 1131-44 (2003).
- [4] T. Starner and J. A. Paradiso, "Human Generated Power for Mobile Electronics", Low Power Electronics Design, Edited by C. Piguet, CRC Press, In press.
- [5] T. von Büren, P. Lukowicz and G. Tröster, "Kinetic Energy Powered Computing – an Experimental Feasibility Study", Proc. 7<sup>th</sup> IEEE Int. Symposium on Wearable Computers (ISWC '03), pp. 22-4, 2003.
- [6] N.M. White, P. Glynne-Jones and S.P. Beeby, "A novel thick-film piezoelectric micro-generator," Smart Mater. Struct., **10**, 850-852 (2001).
- [7] P. Glynne-Jones, M.J. Tudor, S.P. Beeby and N.M. White, "An electromagnetic, vibration-powered generator for intelligent sensor systems," Sensors and Actuators, **A 110**, Issues 1-3, 344-9 (2004).
- [8] P.D. Mitcheson, T.C. Green, E.M. Yeatman, A.S. Holmes, "Architectures for Vibration-Driven Micropower Generators", Journal of MEMS, **13** (3), 429-40 (2004).
- [9] S.P. Beeby, M.J. Tudor, E. Koukharenko, N.M. White, T.O'Donnell, C. Saha, S. Kulkarni, and S. Roy, "Design, fabrication and simulations of microelectromagnetic vibration powered generator for low power MEMS," Accepted Symp on Design Testing Integration and Packaging of MEMS/MOEMS, 01-03 June 2005, Montreux, Switzerland.